

1985-114102

N95-20518

PERFORMANCE, DEFECT BEHAVIOR AND CARRIER ENHANCEMENT IN LOW ENERGY,
PROTON IRRADIATED p⁺nn⁺ InP SOLAR CELLS

I. Weinberg and G.C. Rybicki
NASA Lewis Research Center
Cleveland, Ohio

C. Vargas-Aburto
Kent State University
Kent, Ohio

R.K. Jain
University of Toledo
Toledo, Ohio

and

D. Scheiman
NYMA, Inc.
Brook Park, Ohio

InP p⁺nn⁺ cells, processed by MOCVD, were irradiated by 0.2 MeV protons and their performance and defect behavior observed to a maximum fluence of 10^{13} cm^{-2} . Their radiation induced degradation, over this fluence range, was considerably less than observed for similarly irradiated, diffused junction n⁺p InP cells. Significant degradation occurred in both the cell's emitter and base regions the least degradation occurring in the depletion region. A significant increase in series resistance occurs at the highest fluence. Two majority carrier defect levels, E7 and E10, are observed by DLTS with activation energies at $(E_C - 0.39) \text{ eV}$ and $(E_C - 0.74) \text{ eV}$ respectively. The relative concentration of these defects differs considerably from that observed after 1 MeV electron irradiation. An increased carrier concentration in the cell's n-region was observed at the highest proton fluence, the change in carrier concentration being insignificant at the lower fluences. In agreement with previous results, for 1 and 1.5 MeV electron irradiated InP p⁺n junctions, the defect level E10 is attributed to a complex between zinc, diffused into the n-region from the zinc doped emitter, and a radiation induced defect. The latter is assumed to be either a phosphorus vacancy or interstitial. The increased, or enhanced carrier concentration is attributed to this complex acting as a donor.

INTRODUCTION

The highest AMO efficiency (19.1%) InP solar cell consisted of an n⁺pp⁺ structure epitaxially grown on a p⁺ InP substrate [1]. However, the high cost and relative fragility of InP served as motivation for research efforts directed at heteroepitaxial growth of InP on more viable substrates [2,3]. The highest AMO efficiency (13.7%) for this type of cell was achieved using a GaAs substrate [3,4]. Considering only cost and fracture toughness, Si would be the preferred substrate. The fact that Si is a donor in InP introduces complexities which are necessary in order to avoid the formation of an efficiency limiting counterdiode [5]. One method used to overcome this problem, lies in employing an n⁺p⁺

tunnel junction in contact with the cell's p region. A simpler method consists of using an n⁺ substrate and processing the cell in the p⁺nn⁺ configuration. This eliminates the need for a tunnel junction. Unfortunately, the p/n configuration has received relatively little attention the best cell with this geometry having achieved an efficiency of 17% [6]. Irradiation of these homoepitaxial cells, with 1 MeV electrons, showed that they were slightly more radiation resistant than diffused junction n/p cells [7]. Additional p/n InP cells have been processed by closed ampoule diffusion [8]. Currently, there has been some activity aimed at producing heteroepitaxial p⁺nn⁺ InP cells using n⁺ Ge substrates [9]. Since, like Si, Ge is an n-dopant in InP, use of this configuration obviates the need for a tunnel junction. Obviously, before attempting to process heteroepitaxial cells, one must produce a reasonably good homoepitaxial cell. In the present case we focus our attention on homoepitaxial p⁺nn⁺ cells processed prior to producing the cells heteroepitaxially on an n⁺ Ge substrate [9].

EXPERIMENTAL DETAILS

The cells were processed by MOCVD, at the Spire Corporation, under contract to NASA Lewis. Cell configuration, dopants and concentrations are shown in fig. 1. Processing details can be found in reference 9. Irradiations by 0.2 MeV protons, to a fluence of $10^{13}/\text{cm}^2$ were performed at the University of Michigan's ion implantation facility. Cell performance was determined at NASA Lewis using a Spectrolab Mark II, xenon arc solar simulator with flight calibrated InP standard cell. Spectral response and Isc-Voc measurements were also performed before irradiation and at each step in the irradiation process. Carrier concentrations in the cell's p-base, near the junction were determined by capacitance-voltage measurements. Defect behavior was monitored by DLTS measurements.

RESULTS AND DISCUSSION

Performance

Pre-irradiation performance parameters are shown in table I. Considering the fact that theoretical modelling indicates possible efficiencies over 22%, the present efficiencies are excessively low [10]. This is attributable to the fact that the present cells were processed in an early stage of development. In fact, AMO efficiencies of 17% have subsequently been achieved at Spire [6]. Higher efficiencies can be anticipated with additional effort.

The results of the 0.2 MeV proton irradiations are shown in fig. 2. Comparision of normalized efficiencies with 0.2 MeV proton irradiated diffused junction n/p cells is shown in fig. 3. The n/p cells had the same junction depth as the present cells with AMO efficiency=15.1%, Voc=823 mV, Jsc=29.4 ma/cm², and FF=85.6% [11]. Comparision of normalized efficiencies indicates considerably more radiation resistance for the present cells at the higher fluences. Also, comparing numerical efficiency values, the present cells outperform the n/p cells at the higher fluences.

The external quantum efficiency, before irradiation and at a fluence of 10^{12} cm^{-2} , is shown in fig.4. The quantum efficiency at the highest fluence is lost in the system noise and is therefore not shown in the figure. Figure 4 indicates that considerable degradation occurs in both the emitter and base of the solar cell. A numerical estimate of the relative degradation is obtained using the relation

$$J_{sc} = \sum SR(\lambda_j) E(\lambda_j) \Delta \lambda_j \quad 1a$$

Where $SR(\lambda_j)$ the spectral response, in mA/mW, is obtained from the quantum efficiency using the relation

$$SR(\lambda_j) = Q_E(\lambda_j) \lambda_j / 1.24 \quad 1b$$

where $E(\lambda_j)$ in $\text{mW cm}^{-2} \text{ micron}^{-1}$ is the solar spectral radiance at wavelength λ_j in microns, $Q_E(\lambda_j)$ is the external quantum efficiency at λ_j , $\Delta \lambda_j$ is an appropriate wavelength interval and the summation is over all wavelengths covered by the quantum efficiency in fig.4. The junction depth is approximated by the optical path length l/α_j where α_j is the absorption coefficient at wavelength λ_j . Using 1a and 1b it is found that the degradation in short circuit current is approximately divided between the emitter and base. An estimate of the relative degradation in base and emitter is obtained from the I_{sc} - V_{oc} measurements obtained over a range of light intensities. The results before irradiation and at a specific fluence are shown in table II. Considering the reverse saturation currents J_{02} is attributed to recombination in the cell's depletion region while the major contribution to J_{01} arises from diffusion in the base of the cell. Hence, from the diffusion and recombination current densities in table II, it is concluded that the radiation induced degradation in the cell's base is much greater than that occurring in the depletion region.

Defects

The DLTS spectrum, at the highest fluence, is shown in fig.5 while defect parameters are listed in table III. No defect levels were observed prior to irradiation. The defect concentrations obtained from fig.5, and shown in the table, have been corrected for band bending and its effect on space charge when crossing the Fermi level [12]. The majority carrier defect levels labelled E7 and E10 have been observed previously after irradiation by 1 and 1.5 MeV electrons [13]. The broad signal observed between E7 and E10 appears to be due to the presence of one or more unresolvable defect levels. The present energy levels for E7 and E10 are in reasonable agreement with those previously reported for these defects [13]. However, the concentration ratio $N_T(E10)/N_T(E7) \sim 50$ in the previously electron irradiated case [13] while in the present case the ratio is 0.56. Hence, although E10 could reasonably be assumed to be the major radiation induced defect, observed by DLTS, in the n region of electron irradiated p+n InP [13], the choice of major defect is not clear cut in the present case. It is noted that, after electron irradiation, E7 was observed, but not E10, in

the DLTS spectrum obtained using a Schottky barrier on n-type InP [13]. In fact, E10 was only seen when a p⁺n junction was used, the p⁺ region being heavily zinc doped. It was therefore initially concluded that E10 was a result of zinc diffusion into the n-region, the zinc complexing with an unidentified radiation induced defect [13]. Another possibility considered was the formation of a complex between a process induced and radiation induced defect [13].

Carrier concentrations in the n-region, measured over a range of fluences, indicated that at all but the highest fluence, the change in carrier concentration was negligible. However, at the highest fluence, the carrier concentration was significantly increased over the pre-irradiation value (table IV). This is in opposition to observations in the p-region of n⁺p InP where both proton and electron irradiations produced decreased carrier concentrations [14,15]. Although this appears to be the first reported observation of carrier enhancement in proton irradiated InP, the effect has been observed before after 1 MeV electron irradiation [16]. It is significant that, in both cases, carrier enhancement is observed in the n-region of an InP p⁺n diode where zinc is used as the p-dopant [16]. In agreement with the previous suggestion [13] it was argued that zinc diffuses into the n-region and complexes with a radiation induced defect [16]. In the latter case it was further argued that the defect was either a phosphorus interstitial or vacancy [16]. Furthermore, it was argued that the complex acts as a donor. In relation to the present solar cell parameters, the carrier enhancement does not appear to be a factor in improving cell performance or in decreasing series resistance. This is evident from fig. 1 and table V, the latter showing that cell series resistance, obtained from dark diode I-V data, increases significantly at the highest fluence. In any event, the present results indicate that, despite the anomalous increase in carrier concentration, the effects of radiation induced defects on transport properties, such as diffusion length are dominant in determining cell behavior under the present low energy proton irradiations.

CONCLUSION

Under irradiation by 0.2 MeV protons, it is concluded that;

The radiation induced degradation is considerably lower in the present cell when compared to diffused junction n⁺p InP cells.

Considerable radiation induced degradation is observed in both the base and emitter of the present cells, both degradations being considerably greater than that occurring in the depletion region.

The relative concentration of defects E7 and E10, $N_T(E10)/N_T(E7)$, is considerably greater under 1 and 1.5 MeV electron irradiations than is the case for the present irradiations.

A significant increase in carrier concentration (carrier enhancement) occurs in the cell's n-region after irradiation by 0.2 MeV protons at a fluence of 10^{13} cm^{-2} . At the lower fluences, the change in carrier concentration is insignificant.

In concurrence with previous conclusions after electron irradiation, the defect level E10 is attributable to a donor complex formed between zinc and a radiation induced defect. The latter is assumed to be either a phosphorus interstitial or vacancy.

In the present case, the radiation induced carrier enhancement appears to have little or no effect on cell performance.

REFERENCES

1. C.J.Keavney, V.E.Haven and S.M.Vernon, "Emitter Structures in MOCVD InP Solar Cells," 21st IEEE Photovoltaic Spec. Conf., ppl141-147 (1990)
2. C.J.Keavney, S.M.Vernon and V.E.Haven, "Tunnel Junctions for InP on Si Solar cells," Proceedings Space Photovoltaic Research and Technology Conf., ppl-1 to 1-7, NASA Conf. Publication 3121 (1991)
3. M.W.Wanlass, U.S. Patent No. 4,963,949 (1990)
4. T.J.Coutts, "Progress in InP-Based Solar Cells," Proceedings 3rd Int'l Conf. on InP and Related Materials, pp20-31, IEEE-LEOS, Piscataway N.J. (1991)
5. C.J.Keavney, S.M.Vernon, V.E.Haven, S.J.Wojtczuk and M.M.Al-Jassim, "Fabrication of n^+p InP Solar Cells on Silicon Substrates," Appl. Phys. Lett.54, ppl139-1141 (1989)
6. S.Wojtczuk, S.M.Vernon and E.A.Burke, "p/n InP Solar Cells on Ge Wafers," This Conference (1994)
7. I.Weinberg, C.K.Swartz and R.E.Hart Jr., "Radiation and Temperature Effects in Gallium Arsenide, Indium Phosphide and Silicon Solar Cells," Proceedings 19th Photovoltaic Spec. Conf., pp548-557, IEEE, Piscataway N.J. (1987)
8. Mircea Faur, Maria Faur, C.Goradia, M.Goradia, D.J.Flood, D.J.Brinker, I.Weinberg and N.Fatemi, "Progress in p^+n InP Solar Cells Fabricated by Thermal Diffusion," Proceedings, Space Photovoltaic Research and Technology Conf., pp23-32, NASA Conf. Pub. 3210 (1992)

9. S.Wojtczuk and S.Vernon, "p/n InP Solar Cells on Ge Wafers," Space Photovoltaic Research and Technology Conf. NASA Lewis Res. Center (1994)
10. R.K.Jain, I.Weinberg and D.J.Flood, "Comparative Modelling of InP Solar Cell Structures," Proceedings Space Photovoltaic R and T Conf., pp29-1 to 29-9, NASA Conf. Pub. 3121 (1991)
11. T.Takamoto, H.Okazaki, H.Takamura, M.Ohmori, M.Ura and M.Yamaguchi, "Radiation Effects on n⁺p Homojunction Indium Phosphide Solar Cells," Proceedings 2nd Int'l conf. on InP and Related Materials pp62-65, IEEE-LEOS, Piscataway N.J. (1990)
12. Y.Zohta and M.O.Watanabe, "On The Determination of the Spatial Distribution of Deep Centers in Semiconducting Films From Capacitance Transient Spectroscopy," J. Appl. Phys., 53, pp1809-1811 (1982)
13. J.L.Benton, M.Levinson, A.T.Macrander, H.Temkin and L.C.Kimerling, "Recombination Enhanced Defect Annealing in n-InP," Appl. Phys. Lett., 45, pp566-568 (1984)
14. I.Weinberg, R.K.Jain, C.K.Swartz, H.B.Curtis, D.J.Brinker, C.Vargas-Aburto and P.J.Drevinsky, "Proton Irradiated Heteroepitaxial InP Cells," Proceedings 23rd IEEE Photovoltaic Spec. Conf., pp1483-1486, IEEE, Piscataway N.J. (1993)
15. I.Weinberg, C.K.Swartz and P.J.Drevinsky, "Carrier Removal and Defect Behavior in p-type InP," J. Appl. Phys. 72, pp5509-5511 (1992)
16. A.Sibile, "Origin of the Main Deep Electron Trap in Electron Irradiated InP," Appl. Phys. Lett., 48, pp593-595 (1986)
17. K.Rajkanen and J.Shewchun, "A Better Approach to the Evaluation of the Series Resistance of Solar Cells," Solid State Electronics 22, pp193-197 (1979)

Table I: Cell Pre-Irradiation Performance Parameters

J _{SC}	V _O C	FF	Eff.
mA/cm ²	mV	%	%
23.6	851.4	84.7	12.4

Table II: Diffusion and Recombination Components
of Reverse Saturation Currents

$E_p = 0.2 \text{ MeV}$

Fluence	A_1	A_2	J_{01}	J_{02}
cm^{-2}			A/cm^2	A/cm^2
0	0.89	1.57	1.03×10^{-18}	3.9×10^{-12}
10^{12}	1.32	2.08	1.5×10^{-11}	5.5×10^{-8}

Table III: Characteristics of Majority Carrier Defect
Levels Obtained by DLTS in $p^n n^+$ InP

$E_p = 0.2 \text{ MeV}$
 $\text{Fluence} = 10^{13}/\text{cm}^2$

DEFECT	ACTIVATION ENERGY	CAPTURE CROSS SECTION	CONCENTRATION	INTRODUCTION RATE
	eV	cm^2	cm^{-3}	cm^{-1}
E7	$E_c - 0.39$	4.1×10^{-17}	8.67×10^{15}	867
E10	$E_c - 0.74$	3.6×10^{-14}	4.88×10^{15}	488

Table IV: Electron Concentration in n-Region of 0.2 MeV
Proton Irradiated $p^n n^+$ InP Cell

FLUENCE	ELECTRON CONC.	CHANGE IN ELECTRON CONC. ^a
cm^{-2}	cm^{-3}	cm^{-3}
0	3.18×10^{16}	0
10^{13}	3.86×10^{16}	$+6.8 \times 10^{15}$

^a Change in carrier conc. was negligible at the lower fluence.

Table V: Series Resistance in 0.2 MeV Proton Irradiated Cell

FLUENCE (CM ⁻²)	0	2 X 10 ¹¹	10 ¹²	10 ¹³
SERIES RESISTANCE OHM - cm ²	0.49	0.36	0.56	1.7

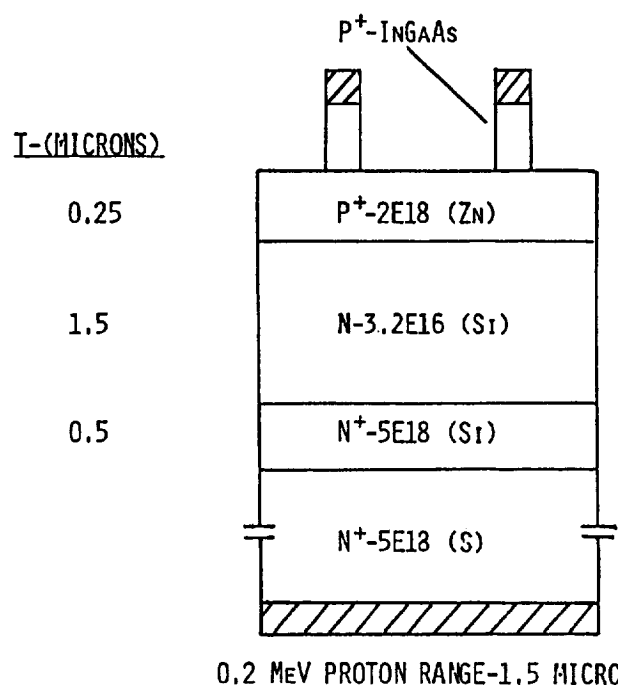


FIGURE 1. InP CELL DETAILS

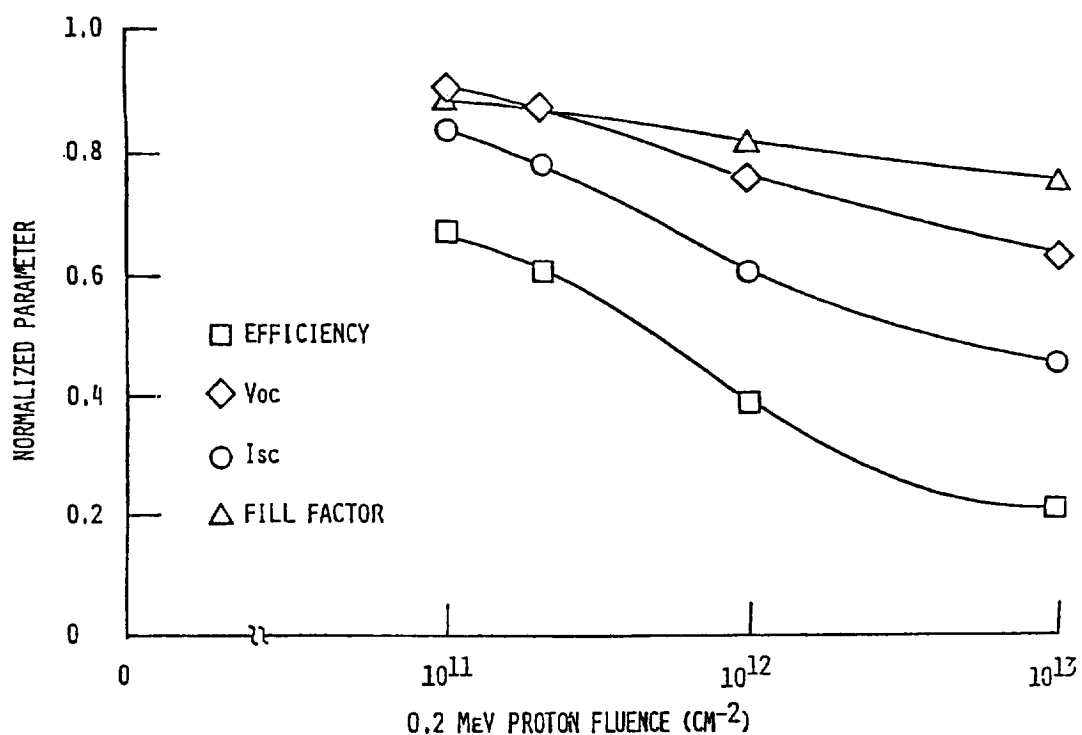


FIGURE 2. NORMALIZED INP CELL PARAMETERS AFTER IRRADIATION

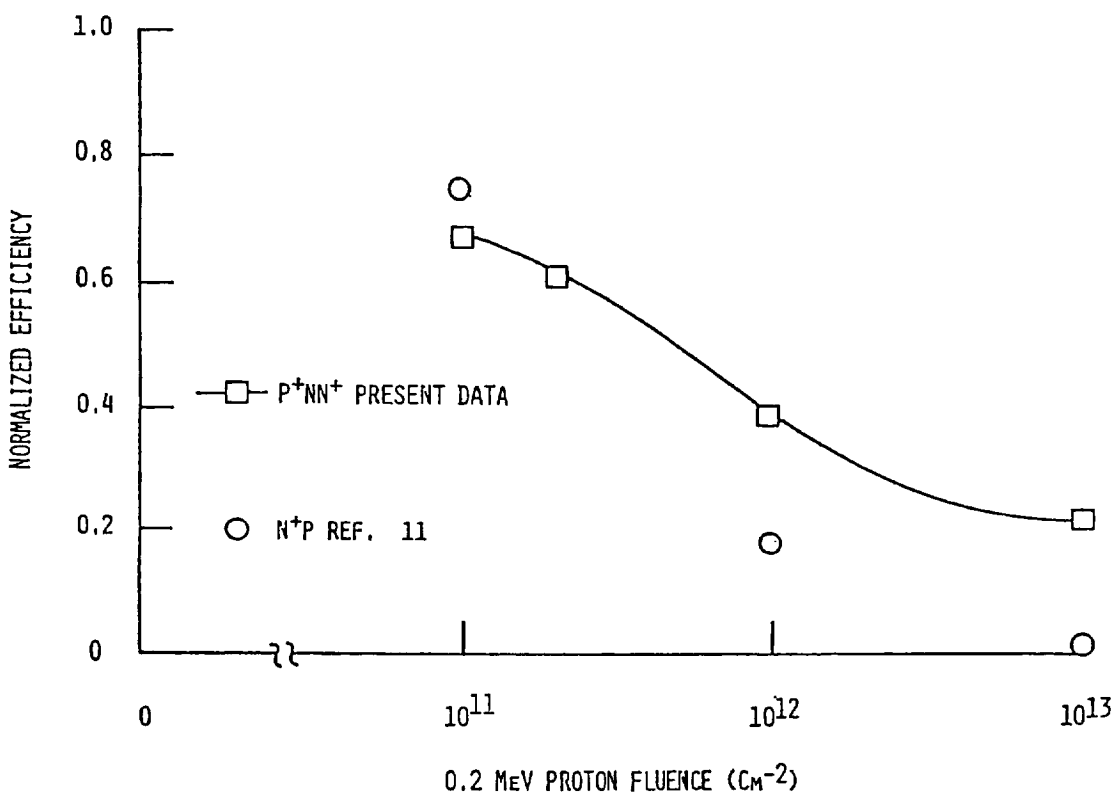


FIGURE 3. COMPARISON OF P⁺NN⁺ AND N⁺P IRRADIATED INP SOLAR CELLS

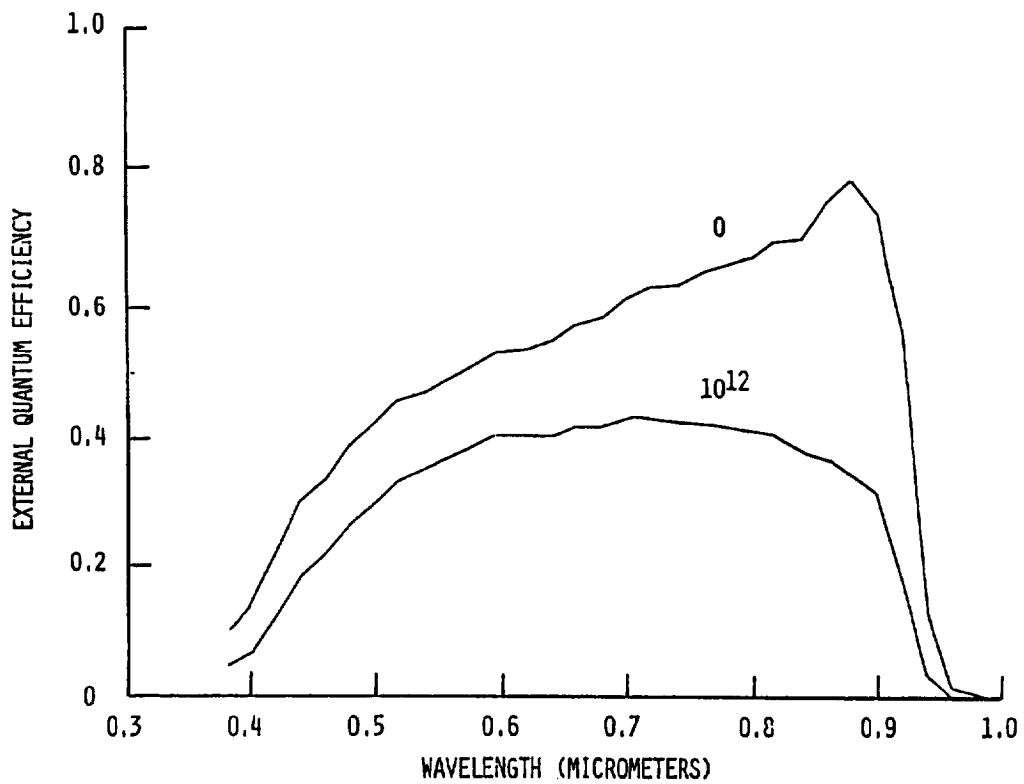


FIGURE 4. EXTERNAL QUANTUM EFFICIENCY, P^+NN^+ INP, $E_p=0.2$ MeV

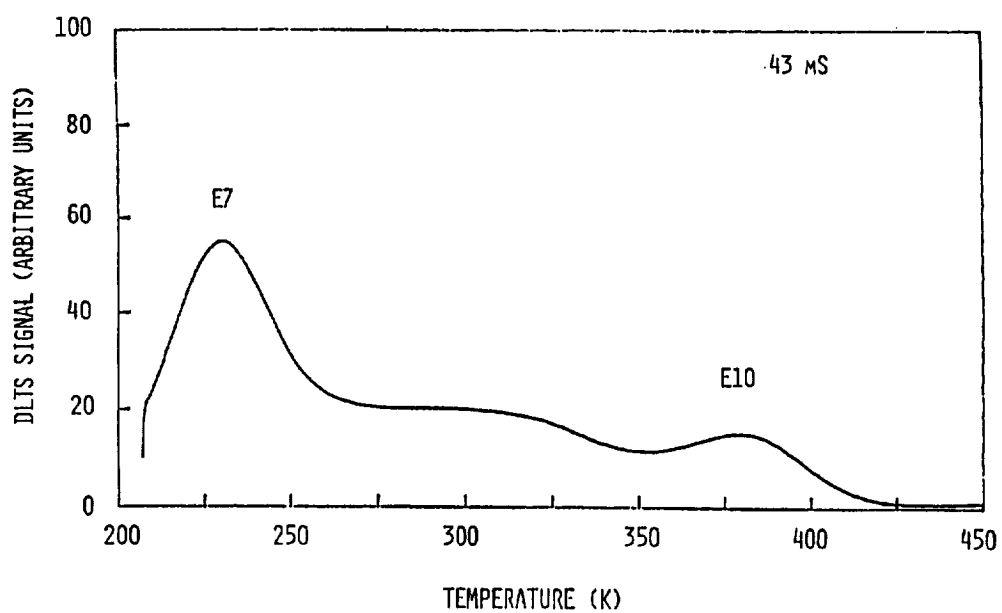


FIGURE 5. DLTS OF P^+NN^+ INP CELL, $E_p=0.2$ MeV, FLUENCE= 10^{13} CM $^{-2}$